

# Time Dependent Model for Non-Inductive ECH X-I Current Ramp-Up for SHPD Tokamak Facility

Masayuki Ono<sup>a</sup>, Nicola Bertelli, and Syunichi Shiraiwa

*Princeton Plasma Physics Laboratory, Princeton, NJ, 08540, USA*

*<sup>a</sup>Corresponding Author: mono@pppl.gov*

**Abstract.** Non-inductive (NI) plasma current start-up and ramp-up is an important research topic for spherical tokamak (ST) based reactors and fusion pilot plant (FPP). For a compact FPP, the OH flux availability is highly restricted due to its compact geometry. In Ref. [1], efficient fundamental extraordinary mode (X-I) electron cyclotron heating (ECH) current start-up and ramp-up regime was identified for a reactor-like high toroidal magnetic field range which has more than a hundred times higher current drive efficiency compared to more conventional ECH methods for the relevant start-up temperature range. High current drive efficiency is possible due to the strong X-I fundamental ECH interaction only with unidirectional passing electrons constrained by the wave accessibility conditions. Here, we extend the X-I electron cyclotron current drive (ECCD) investigation to a time dependent model to simulate the non-inductive current ramp-up to 10 MA for the Sustained High Power Density (SHPD) facility. As the X-I ECCD driven current  $I_{EC}$  rises, due to the back EMF driven negative current, the net plasma current  $I_p$  rises more slowly with the current resistive time scale. For tokamak confinement time (both L-mode and H-Mode) which tends to rise with  $I_p$ , a positive feedback results and even with constant applied ECH power,  $T_{e0}$ ,  $I_{EC}$ , and  $I_p$  can continue to rise to very high values. However, in a realistic situation, the  $T_{e0}$  rise should saturate due to a number of factors such as enhanced core radiation and increased power loss at high temperature. To simulate this effect, we adopt a maximum  $T_{e0}$  model which would limit the temperature rise to certain  $T_{e0}$ . With this model, we investigated the current ramp-up for various ECH power levels and the maximum  $T_{e0}$  of 15, 20, and 25 keV. We find that while the power required is reduced with increasing  $T_{e0}$  limit due to increased current drive efficiency, the time to reach 10 MA tends to go up due to the reduced plasma resistivity for the higher  $T_{e0}$  limit. We also find for a given  $T_{e0}$  limit, the time to reach 10 MA tends to be reduced by increasing the applied ECH power by over driving the current ramp-up where  $I_{EC}$  is driven at significantly higher level than 10 MA. While the current ramp-up time may not be an issue for the steady-state reactor systems, if it is desirable to minimize the current ramp-up time, it is prudent to have a sufficient ECH power for current over-drive and have some  $T_{e0}$  limiting tools such as impurity seeding for enhanced radiation. A well-controlled NI ECH start-up also has a potential of improving the tokamak start-up reliability and avoid run-away electrons while the NI off-axis current drive could enhance MHD stability and plasma performance improvements.

## INTRODUCTION

Motivation for non-inductive (NI) current start-up and ramp-up is quite well known for spherical tokamaks (STs) as the inner high field core region is generally highly constrained for incorporating a high performance central solenoid (CS). ST is attractive for its high beta stability property needed for economical fusion reactors [2]. In the recent years, a compact cost-effective fusion pilot plant (FPP) is viewed as an important next step for the fusion reactor development path [3-6]. Recent advances in high temperature superconducting magnet technology allow realization of compact high toroidal field (TF) magnets even for lower aspect-ratio reactor systems. If the CS could be indeed eliminated or significantly reduced, the optimization process of FPP is greatly simplified as the design no longer needs to find the valuable central space for CS and to deal with the serious coil stresses arising from the JxB force interaction of CS-TF coils. There are many possible CS-free tokamak start-up methods which were successfully investigated as summarized in Ref. [2]. Among various start-up methods, the ECH-based start-up appeared to be attractive for reactor application [7 - 13]. Recently, it was shown via modelling that the X-mode resonance at  $\omega = \Omega_e$  (X-I) has an

exceptionally high ECH and ECCD efficiencies even at the low start-up temperature of sub-keV range for reactor-like high toroidal field systems  $\sim 5\text{-}6\text{ T}$  [1]. In this paper, we extend the previous work to a time dependent model to show it is indeed possible to ramp-up the plasma current to 10 MA utilizing  $\sim 10\text{ - }20\text{ MW}$  of X-I ECH power for the Sustained High Power Density (SHPD) tokamak facility parameters.

## X-I ACCESSIBILITY CONDITIONS

Here we briefly review the X-I accessibility condition. It is well known that the X-mode launched from the low-field-side (LFS) toward the electron cyclotron fundamental resonance  $f = f_{ce}$  is reflected at  $n_{\parallel}^2 = R \equiv 1 - f_{pe}^2 / (f(f - f_{ce}))$  cut-off layer which is located at the LFS of the  $f = f_{ce}$  resonance so the wave actually cannot reach the resonance. However, if the wave fundamental Doppler resonance condition  $(\omega - \Omega_e) / (k_{\parallel} V_{e0}) \leq 3$  is satisfied before reaching the  $n_{\parallel}^2 = R$  reflection layer, the fundamental resonant interaction can take place. This resonance condition together with the  $n_{\parallel}^2 = R$  cut-off condition yields the following  $f = f_{ce}$  or X-I resonance accessibility condition:

$$n_{ea} \leq 37.5 f^2 \frac{V_{e0}}{c} n_{\parallel} (1 - n_{\parallel}^2) \quad (1)$$

where the accessible density  $n_{ea}$  in the unit of  $10^{19}/\text{m}^3$  is relatively insensitive to  $n_{\parallel}$  but depends strongly as  $\propto f^2$  or  $B_{T0}^2$  where  $f$  is the wave frequency in the unit of 100 GHz. Since  $n_{ea}$  goes up with  $f^2$ , the higher frequency (or higher toroidal field) such as 170 GHz helps to satisfy the accessibility condition. The accessibility also improves for higher  $V_{e0}$  or  $T_{e0}$ . The insensitive  $n_{\parallel}$  dependence allows the use of a simple waveguide launcher. Fig. 1 illustrates the effectiveness of X-I ECH and ECCD for a typical start-up density of  $0.5 \times 10^{19}/\text{m}^3$  for various representative start-up temperature of  $T_{e0} = 200, 500,$  and  $800\text{ eV}$ . Here the wave resonance layer position  $f = f_{ce}$  is fixed at  $R = 1\text{ m}$  with the  $B_{T0}$  scan. The launched wave parallel index of refraction is  $n_{\parallel 0} = 0.4$  which is equivalent to  $24^\circ$  of wave injection angle. In Fig. 1(a), single path fractional absorption  $P_{ECH}/P_0$  is plotted for X-I ECH. For the X-I ECH, the fractional power absorption drastically increases from zero (no absorption) to one (full absorption) as the toroidal magnetic field is increased. The ‘‘transition’’ magnetic field is higher for lower  $T_{e0}$  due to the accessibility condition described above. But even at low-end temperature of  $200\text{ eV}$ , full absorption can be achieved with  $B_{T0} \sim 5\text{-}6\text{ T}$  toroidal field which is the toroidal magnetic field of typical fusion reactor systems such as ITER and FPPs. The efficient cyclotron absorption at the low temperature is possible as the X-mode polarization can directly interact with the electron gyro-motion without requiring finite-Larmor-radius (FLR) effects. The corresponding ECH absorption for the second harmonic X-mode (X-II) using twice the frequency is shown in Fig. 1(a) which is an order of magnitude smaller. In Fig 1(b), the corresponding ECCD current ( $I_{ECCD}$ ) is shown. The X-I  $I_{ECCD}$  increases with  $T_{e0}$  but remains quite efficient even for low-end temperature of  $T_{e0} = 200\text{ eV}$  at  $B_{T0} = 5\text{-}6\text{ T}$ . The corresponding X-II  $I_{ECCD}$  amplified by  $\times 100$  is much smaller as shown in Fig. 1(b).

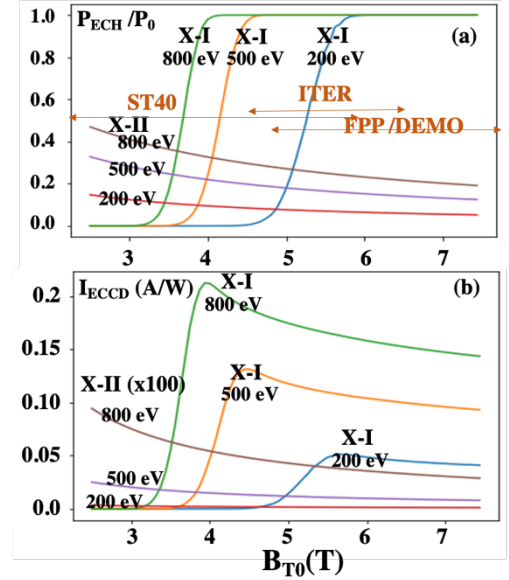


**FIGURE 1.** ECH and ECCD as a function of  $B_{T0}$ .  $R = 1\text{ m}$ ,  $n_{\parallel 0} = 0.4$ ,  $n_{e0} = 0.5 \times 10^{19}/\text{m}^3$  and  $T_{e0}$  as labeled. (a) Fractional ECH for X-I and IX-I. (b) Corresponding ECCD for X-I and IX-I.

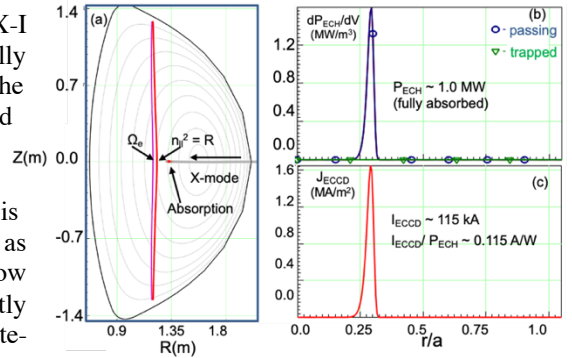


**FIGURE 2.** Propagation, absorption and current drive of X-mode in SHPD with  $R = 1.58\text{ m}$ ,  $R/a \sim 2$ ,  $B_{T0} = 5\text{ T}$ ,  $n_{e0} = 10^{19}/\text{m}^3$  and  $T_{e0} = 1\text{ keV}$ , using TRAVIS code. (a) A poloidal cross-section of the LFS X-mode propagation. The power absorption region is indicated in red. (b) Power absorption radial profile. (c) Driven current density profile.

## TIME DEPENDENT MODEL OF X-I ECCD NON-INDUCTIVE CURRENT RAMP-UP

For the time dependent model of the X-I ECCD current ramp-up, the following equation was used:

$$V_l = I_B R_B + L_B \frac{dI_B}{dt} + M_{EC} \frac{dI_{EC}}{dt} \quad (2)$$

where  $I_{EC}$  is the current driven by ECCD and  $I_B$  is the induced negative current by back EMF as the plasma responds to rising  $I_{EC}$ .  $M_{EC}$  is the mutual inductance between ECCD current  $I_{EC}$  and induced plasma current  $I_B$ .  $R_B$  is the plasma resistivity for the induced current and  $L_B$  is the plasma inductance of induced current, and  $V_l$  is the loop voltage which is zero for the present NI plasma ramp-up study. Utilizing Eq. (2), it is straight forward to have non-zero  $V_l$  to simulate the inductive ramp-up scenarios. One might note here that for the inductive ramp-up case, one can envision using ECH and ECCD to assist the inductive start-up such as the case for ITER. For this paper however, we shall focus solely on the NI current ramp-up with  $V_l = 0$ . As  $I_{EC}$  is ramped-up, the induced plasma current  $I_B$  tends to shield  $I_{EC}$ , i.e.,  $\frac{dI_B}{dt} \sim -\frac{dI_{EC}}{dt}$ , we let  $L_B \sim M_{EC}$  as both currents are expected to flow in the same plasma region. For tokamak plasma, the plasma inductance  $L_B = \mu_0 R (\ln 8R/a + l_E/2 - 2)$  where  $l_E$  is the internal inductance and it is  $\sim 0.5$  for a uniform current profile and the plasma resistivity  $R_B = 5 \times 10^{-7} \ln \Lambda Z_B (2R/a^2) T_e^{-3/2}$  where  $R$  is the major radius and  $a$  is the minor radius. In the present time dependent model, we prescribe the plasma density time evolution  $n_{e0}(t)$ , and plasma size evolution for  $R(t)$ ,  $a(t)$ , and elongation  $\kappa(t)$ .  $Z_B$  is the effective plasma resistivity which we assume here conservatively to be 4 for this simulation.  $Z_B$  affects both plasma resistivity as well as the ECCD current drive efficiency. For the term  $T_e$  in the plasma resistivity term, we use the volume averaged temperature in this model. The  $T_e$  term is important for the ECCD current drive efficiency as well as the plasma resistivity determining the NI current ramp-up time. Here we used a peaked  $T_e$  profile of  $T_e(r) = (T_{e0} - T_{ee})(1 - (r/a)^2)^3 + T_{ee}$  and the edge temperature  $T_{ee}$  is 1/100 of the central temperature  $T_{e0}$ . The peaked  $T_e$  profile tends to reduce the current drive efficiency, but it may simulate well the L-mode type discharges. As the induced  $I_B$  decays resistively through the  $I_B R_B$  term, the net current  $I_p = I_{EC} + I_B$  appears. In each time step, the RT-4 [13] is used to calculate the EC ray-trajectories which yields the absorbed ECH power  $P_{ECH}$  and resulting ECCD current  $I_{EC}$ . We note that RT-4 has been benchmarked previously with the GENRAY [14] and TRAVIS [15] codes [1, 9, 13]. The plasma current  $I_p$  determines the tokamak performance and it will be used to evaluate the plasma confinement time. In this analysis, the L-mode scaling [16] can be used to estimate the L-mode confinement time  $\tau_{97L}$  of the plasma. It should be noted that the L-mode confinement behavior is shown to be very robust, observed in a variety of auxiliary heated tokamak plasmas including ECH as described in Ref [16]. From  $\tau_{97L}$  and  $P_{ECH}$ , one can obtain new plasma pressure. Since the plasma density  $n_{e0}$  is specified, one can obtain new  $T_{e0}$ . With new  $T_{e0}$ , one can then run the next ray-tracing and obtain new  $P_{ECH}$  and  $I_{EC}$ . A schematic of the time dependent model of X-I current ramp-up is shown in Fig. 3. The ECH heating power  $P_{ECH}$  raises electron plasma pressure,  $\Delta p_{e0}$ . With constant plasma density, the electron plasma pressure rise would increase electron temperature  $\Delta T_{e0}$ . The increased  $\Delta T_{e0}$  increases the ECCD current drive  $\Delta I_{EC}$  as the current drive efficiency tend to increase with  $T_{e0}$ . The increased ECCD current drive increases the plasma current  $\Delta I_p$ . Finally, the increased plasma current increases the plasma confinement time completing the positive feedback heating and current drive cycle. Since the confinement time increases with the plasma current is true for all of the tokamak-based plasma confinement scalings for both L and H-modes, this positive feedback cycle is naturally expected for a tokamak system. One should also note here that for X-I, the ECH absorption should be 100% throughout the start-up and ramp-up path, therefore  $P_{ECH}$  is essentially the same as the injected ECH power.

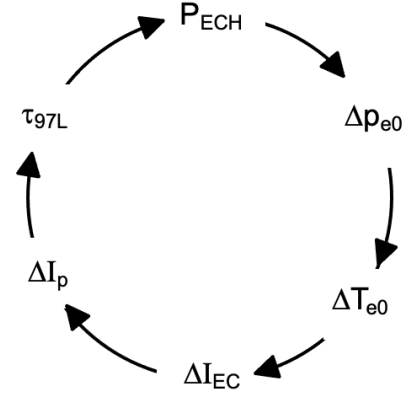


**FIGURE 3.** Time dependent model of X-I current ramp-up. The ECH heating power  $P_{ECH}$  raises electron plasma pressure,  $\Delta p_{e0}$ . With constant plasma density,  $\Delta p_{e0}$  increase would increase electron temperature  $\Delta T_{e0}$  which increases  $\Delta I_{EC}$  resulting in increased  $\Delta I_p$ . Finally, the increased  $\Delta I_p$  increases  $\tau_{97L}$  completing the positive feedback cycle.

## NON-INDUCTIVE CURRENT RAMP-UP OF SHPD PLASMA

In Figure 4, an example of the current ramp-up time evolution is shown for the SHPD parameters. As shown in the figure,  $I_{EC}$  ramps up rapidly due to the positive feedback cycle. As  $I_{EC}$  ramps up, there is also a similar level of negative current due to the back EMF. The net plasma current  $I_p$  therefore rises more slowly with the current resistive time over a span of  $\sim 350$  sec as shown Fig. 4(a). The ECH power is assumed to ramp-up from 1 MW to 10 MW initially, then kept constant as shown in Fig. 4(b). The initial time step is 2 msec which is increased to 50 msec at the end of the ramp-up period then the 50 msec time step is maintained for the rest of the discharge evolution. In Fig. 4(c), the normalized confinement time evolution is shown. The  $\tau_E$  is required confinement time to maintain the plasma stored energy with the absorbed ECH power  $P_{ECH}$ . As shown in Fig. 4(c),  $\tau_{97L}$  is always larger than  $\tau_E$  which is required for the power balance point of view. As shown in the figure, in the early phase,  $\tau_{97L}$  remains well above  $\tau_E$ , showing that there is an ample power to provide extra heating for the current ramp-up. The plasma density is assumed to be controlled as shown in Fig. 4(d) where the density starts at  $0.5 \times 10^{19}/m^3$  and ramped up to  $1 \times 10^{19}/m^3$ . In Fig. 4(e),  $T_{e0}$  time evolution is shown which increases unchecked to over 100 keV and because of the high  $T_{e0}$ , the plasma current rises very slowly (due to the low resistivity) not quite reaching the steady-state even for the time duration of 350 sec.

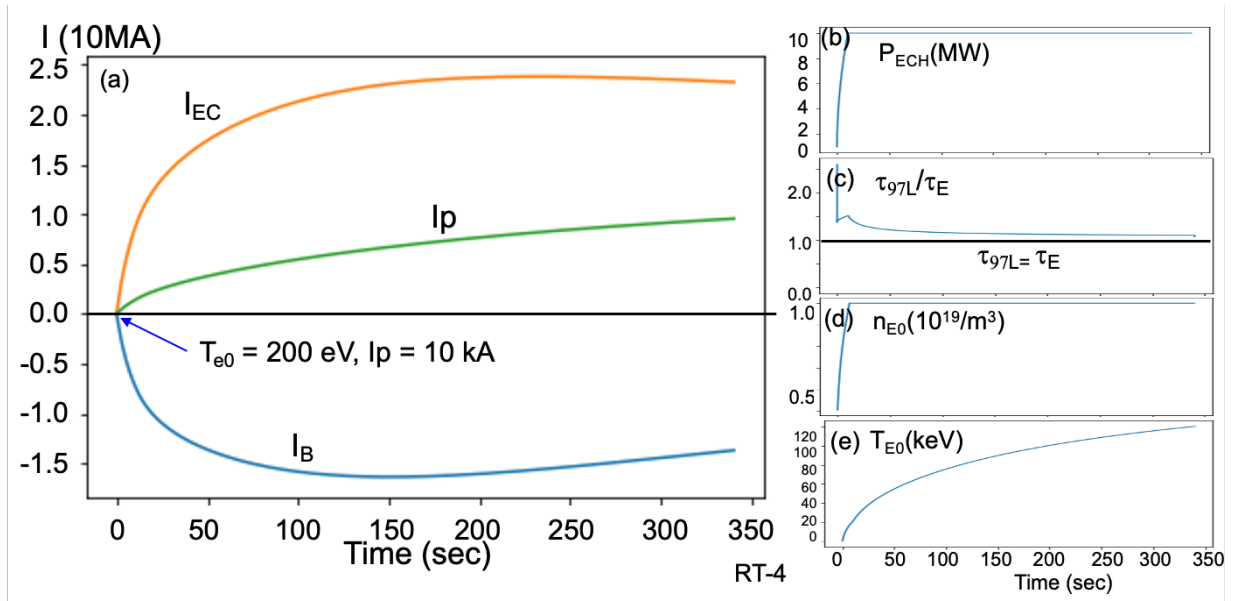


**FIGURE 4.** Time evolution of X-I  $I_{ECCD}$  for  $n_{||0} = 0.4$  utilizing the ITER 97 L-mode confinement scaling. (a)  $I_{EC}$  is the ECCD driven current,  $I_B$  is the back EMF induced negative current, and  $I_p$  is the net plasma current. The plasma current starts at 10 kA. (b) Applied ECH power evolution with 1 MW initially and ramping up to 10 MW. (c) Normalized confinement time  $\tau_{97L}/\tau_E$  evolution. (d) Central density evolution starting at  $0.5 \times 10^{19}/m^3$  ramping up to  $1 \times 10^{19}/m^3$ . (e)  $T_{e0}$  evolution with initial value of 200 eV.

As shown in Fig. 4 with unchecked rising  $T_{e0}$  case, it may not be realistic to assume that  $T_{e0}$  can keep increasing without limit. While we do not know the actual transport behavior at high  $T_{e0}$ , it is prudent to assume that some kind of temperature saturation will occur at high  $T_{e0}$ . We should note that  $\tau_{97L}$  does not contain electron temperature saturation or confinement degradation at high  $T_{e0}$  due to the relatively small experimental confinement data base. The plasma radiations at high  $T_{e0}$  are also likely to cause increased plasma energy losses and  $T_{e0}$  saturation. For this reason, we run the simulation code to include the  $T_{e0}$  saturation. In Fig. 5, a case of  $T_{e0}$  saturation at  $T_{e0} = 25$  keV is shown. Once  $T_{e0}$  saturates,  $I_{EC}$  also saturates and  $I_B$  is no longer driven by the back EMF and it decays resistively with  $L_B/R_B$  time as can be seen in Fig. 5(a). Once  $I_p$  rises to 10 MA, we apply the  $P_{ECH}$  feedback control to maintain  $I_p$  at 10 MA as shown in Fig. 5(b).  $\tau_{97L}$  remains well above  $\tau_E$  as shown in Fig. 5(c). The density evolution shown in Fig. 5(d) is the same as the case shown in Fig. 4. The corresponding  $T_{e0}$  evolution is shown in Fig. 5(e). This  $T_{e0}$  saturation also enables the discharge to ramp-up to 10 MA in a reasonable time of  $\sim 280$  sec.

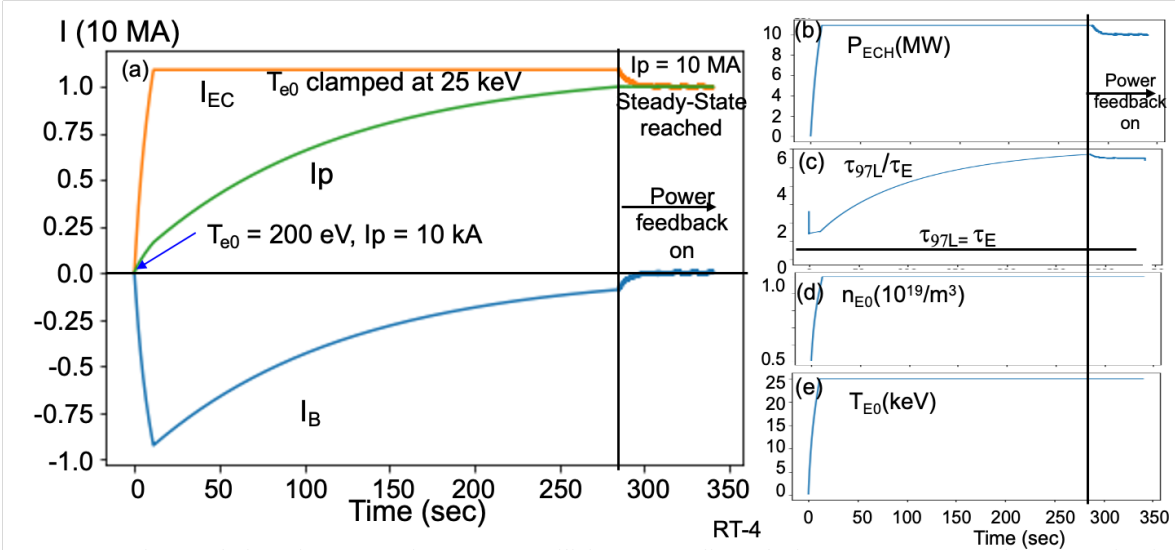


**FIGURE 5.** Time evolution of X-I  $I_{ECCD}$  for  $n_{||0} = 0.4$  utilizing  $\tau_{97L}$  scaling. The input parameters are the same as in Fig. 4 except for the maximum  $T_{e0}$  is assumed to be 25 keV and feedback control applied once  $I_p$  reaches 10 MA.

We shall now investigate the NI current ramp-up time as a function of applied ECH power and the level of temperature saturation as shown in Figs. 6 – 8. In Figs. 6 - 8, the NI current ramp-up for various applied  $P_{ECH}$  as labeled is shown for the saturation temperatures of 25 keV, 20 keV, and 15 keV, respectively. As can be seen from the figures, the ramp-up time is shorter for higher power due to the current over-drive effect where  $I_{EC}$  is much larger than the target 10 MA. As shown in Fig. 6, by increasing the power from 11 MW to 13 MW, the rise time is shortened by  $\sim 100$  sec. Similar behavior can be seen for the lower temperature cases shown in Figs 7 and 8. The lower saturation temperature tends to increase the required ECH power due to lower ECCD efficiency but the current ramp-up time tends to decrease due to the increased plasma resistivity. These cases suggest something like an impurity seeding, if needed to shorten the current ramp-up time, maybe an effective way to limit the maximum  $T_{e0}$  via enhanced radiation to reduce the ramp-time if sufficient ECH power is available.

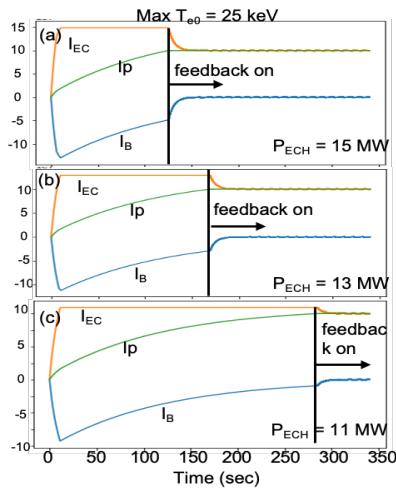


**FIGURE 6.** The ECH power dependence of the current ramp-up time with the  $T_{e0}$  saturation of 25 keV. (a)  $P_{ECH} = 15$  MW. (b)  $P_{ECH} = 13$  MW. (c)  $P_{ECH} = 11$  MW.

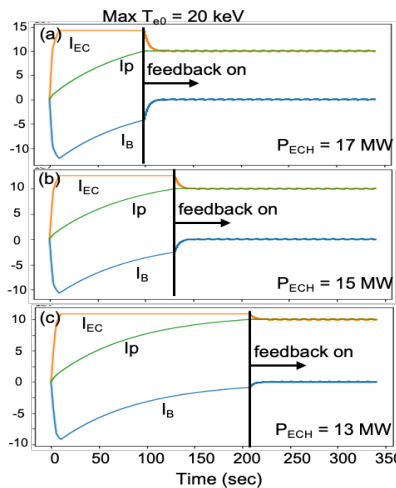


**FIGURE 7.** The ECH power dependence of the current ramp-up time with the  $T_{e0}$  saturation of 20 keV. (a)  $P_{ECH} = 17$  MW. (b)  $P_{ECH} = 15$  MW. (c)  $P_{ECH} = 13$  MW.

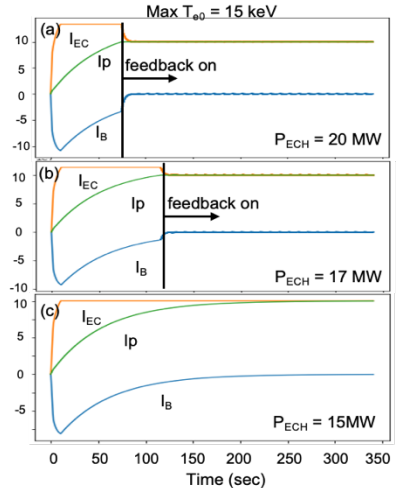


**FIGURE 8.** The ECH power dependence of the current ramp-up time with the  $T_{e0}$  saturation of 20 keV. (a)  $P_{ECH} = 20$  MW. (b)  $P_{ECH} = 17$  MW. (c)  $P_{ECH} = 15$  MW.

## CONCLUSION

A time dependent model of NI start-up of X-I ECCD has been developed. The X-I with a strong ECH absorption even at low electron temperature regime of initial start-up plasma makes the efficient NI start-up and current ramp-up possible. The parameter of the SHPD tokamak facility was used to investigate the current ramp-up to 10 MA from 10 kA, 200 eV initial plasma with  $\sim 10 - 20$  MW of ECH power. The  $I_{EC}$  ramps up rapidly but induces the similar level of back EMF negative current resulting in the net plasma current  $I_p$  rising more slowly with the current resistive time scale. Since our objective is to reach  $I_p = 10$  MA, one can envision a current feedback control once  $I_p = 10$  MA is reached. For the present simulation, we assumed the plasma R, a, and elongation  $\kappa$  are held constant. We have also run cases with smaller plasma size with increasing in size as the plasma current rises. The smaller initial plasmas tend to reduce the ECH power requirements so one could start the plasma with lower power which might be a good strategy from the machine safety point of view. The larger confinement factor  $\tau_{97L}/\tau_E > 2.0$  also alleviates concerns of possible worse than  $\tau_{97L}$  confinement behavior at the initial start-up stage. Since the plasma confinement scaling typically do not contain temperature confinement degradation, the time dependent model with  $\tau_{97L}$  tends to cause uncontrolled  $T_{e0}$  rise. As such a case is likely unrealistic, we run some cases with maximum  $T_{e0}$  limiting cases for various heating power. Among three  $T_{e0}$  limits of 25, 20, and 15 keV, higher  $T_{e0}$  limit tends to reduce the required ECH power but it also tends to increase the ramp-up time due to lower plasma resistivity. Higher power  $P_{EC}$  would over drive the  $I_{EC}$  well over 10 MA which would reduce the ramp-up time. We used here a relatively conservative  $Z_B$  of 4. If lower  $Z_B$  is possible, it has similar effects as increased  $T_{e0}$  which would increase the current drive efficiency but also reduces the plasma resistivity which could slow down the current ramp-up rate. One could thus use an impurity injection as a tool to limit the  $T_{e0}$  rise and reduce the current ramp-up time if needed. The NI current ramp-up scenarios to 10 MA in the SHPD tokamak facility therefore appears to be relatively robust with  $P_{EC}$  of 10 – 20 MW range for the SHPD facility. The present NI X-I current ramp-up method could be also applied to ITER start-up as it could eliminate the initial loop-voltage spike and make the start-up more reliable and controllable while avoiding the run-away electrons. It could be also used for the current profile control to enhance plasma MHD stability and performance. The present NI X-I ECH start-up and ramp-up can be tested in any tokamaks/STs with sufficient toroidal magnetic field strength to have the fundamental electron cyclotron resonance within the plasma. A feasibility study was recently performed for the ST-40 high field ST [17] where the MW-class  $f = 105/140$  GHz gyrotron system is being implemented.

## ACKNOWLEDGMENTS

This work supported by DoE Contract No. DE-AC02-09CH11466.

## REFERENCES

1. M. Ono et. al., *Physical Review E* 106, L023201 (2022).
2. M. Ono and R. Kaita, *Physics of Plasmas* **22**, 040501 (2015).
3. see for example, [https://usfusionandplasmas.org/FESAC\\_Report\\_2020\\_Powering\\_the\\_Future.pdf](https://usfusionandplasmas.org/FESAC_Report_2020_Powering_the_Future.pdf), and <https://www.nap.edu/read/25991/chapter/1>
4. J.E. Menard, et al, *Nucl. Fusion*, **56** 106023 (2016).
5. R.J. Buttery, et al, *Nucl. Fusion*, **61** 046028 (2021).
6. J.E. Menard, et al, *Nucl. Fusion*, **62** 036026 (2022).
7. C.B. Forest, Y-S Hwang, M. Ono, and D.S. Darrow, *Phys. Rev. Lett.* **68** 3559 (1992).
8. T. Yoshinaga, et al., *Phys. Rev. Lett.* **96**, 125005 (2006).
9. H. Idei et al., *Nucl. Fusion* **57** 126045 (2017).
10. M. Ishiguro, et al., *Physics of Plasmas* **19**, 062508 (2012).
11. V.F. Shevchenko, et al., *Nucl. Fusion* **50** 022004 (2010).
12. Kojima S., et al., *Plasma Phys. Control. Fusion* **63** 105002 (2021).
13. M. Ono, et al., *AIP Conference Proceedings* **2254** (2020) 090001.
14. N.B. Marushchenko et al, *Comp. Phys. Comm.* **185** (2014) 165.
15. A.P. Smirnov, R.W. and Harvey, *Bull. Am. Phys. Soc.* **40** (1995) 1837.
16. S. M. Kaye et al., *Nucl. Fusion* **37** 1303 (1997).
17. M. Ono et al., *Nucl. Fusion* **62** 106035 (2022).